Eastern North Atlantic Mode Waters during POMME (September 2000-2001)

Gilles Reverdin, Michel Assenbaum, Louis Prieur

Eastern North Atlantic Mode Waters during POMME (September 2000–2001)

G. Reverdin

Laboratoire d'Océanographie Dynamique et de Climatologie, Institut Pierre-Simon Laplace, Centre National de la Recherche Scientifique, Paris, France

M. Assenbaum

Laboratoire d'Etudes en Géophysique et Océanographie Spatiales/Observatoire Midi-Pyrénées, Service Hydrologique et Océanographique de la Marine, Toulouse, France

L. Prieur

Laboratoire d'Océanographie de Villefranche, Centre National de la Recherche Scientifique, Villefranche-sur-mer, France

Received 21 July 2004; revised 8 April 2005; accepted 17 May 2005; published 9 July 2005.

[1] Four hydrographic surveys in the northeast Atlantic (38°–45°N, 15°–21°W) carried out during the Programme Océan Multidisciplinaire Méso Echelle (POMME) experiment (September 2000–2001) are used to investigate the water masses in the upper layers corresponding to Eastern North Atlantic Mode Waters. A large meridional gradient in isopycnal temperature/salinity is witnessed which has no counterpart in climatology and is associated with an anomalous eastward current near 41°N. Waters tend to be warmer/more salty, somewhat more stratified, and less oxygenated on isopycnal surfaces in the southern part of the domain. In addition, there is an overlying zonal gradient of properties, in particular, north of the jet, consistent with earlier descriptions. However, these large-scale distributions also change significantly through the POMME year, in particular, between the February and early April surveys, which we attribute to (1) the arrival of a 2001 vintage of mode waters, in particular, in the northeastern part of the domain and to (2) stirring by the mesoscale motions, which contribute to down-gradient transport (equivalent diffusion coefficient of 2000 m^2/s for $\sigma = 27.10$). On a smaller scale, there are noticeable changes in properties between surveys, some of which can be shown by quasi-Lagrangian diagnostics to result from advection by the horizontal circulation. In particular, in the southwest corner of the domain between the surveys P1 (February 2001) and P2 (April 2001), horizontal isopycnal advection is responsible for a large cooling (freshening) and oxygen increase, or in the northeast corner, where new oxygenated and freshly ventilated water (in particular for surface $\sigma_\Theta = 27.05$ kg/m^3) penetrates during that period. In other regions, or for a longer period, water masses are often difficult to track as a result of dispersion or stirring by the eddies and too small of a POMME domain.

Citation: Reverdin, G., M. Assenbaum, and L. Prieur (2005), Eastern North Atlantic Mode Waters during POMME (September 2000–2001), *J. Geophys. Res.*, *110*, C07S04, doi:10.1029/2004JC002613.

1. Introduction

[2] The average circulation in the northeast Atlantic near 35°–45°N is often portrayed as having southward currents in the upper ocean layers [*Paillet and Mercier*, 1997]. This is consistent with the southward spreading of a low-stratification layer (a light variety of subpolar mode water referred to as Eastern North Atlantic Mode Water (ENAMW)) centered on the potential density surface $\rho_\theta = 1027.10$ kg/m^3 [*Paillet and Arhan*, 1996] (later on, ispopycnal surfaces will be reported by $\sigma_\theta = \rho_\theta - 1000$ kg/m^3, where ρ_Θ is potential density referred to the sea surface pressure). This circulation might not be always present (for example, the analysis of the Vivaldi 1991 data set presents a northeastward flow to the northwest of 18°W/44°N and a very weak return southward flow to its east [*Pollard et al.*, 1996; *Cunningham*, 2000; *Leach et al.*, 2002]). In the late 1980s and 1990s, oxygen and stratification reported on potential density surfaces of the upper ocean presented an average meridional gradient in the northeast Atlantic, whereas salinity presented a zonal gradient [*Perez et al.*, 1995; *van Aken*, 2001]. According to *van Aken*'s [2001] study, the zonal salinity gradient exceeds interannual variability, although the information on interannual variability is based on fairly localized data (mostly close to the Iberian peninsula; for salinity, see *Perez et al.* [1995]) or with poor time resolution [*Pollard and Pu*,

0148-0227/05/2004JC002613

1985]. Modeling studies, for example *Valdivieso da Costa et al.* [2005], illustrate that the minimum potential vorticity and formation rates of ENAMW vary considerably from year to year in this region. Are the property gradients found in earlier surveys still present in more recent years; can we progress on testing the dynamical processes involved in their maintenance? To answer these questions, we rely on information on the circulation and hydrological surveys collected during the Programme Océan Multidisciplinaire Méso Echelle (POMME) (September 2000–2001).

[3] In the POMME region located between 45°N and the Azores Current to the south, the average southward circulation is O(1 cm/s) whereas the eddy structures have velocities of O(10 cm/s) according to satellite altimetry which characterizes this region as a rather quiescent area [*Ducet et al.*, 2000; *Volkov*, 2004]. These eddy motions have been shown during Vivaldi 1991 to provide an important contribution to meridional transport of heat, salt and potential vorticity [*Leach et al.*, 2002]. The respective role of the average circulation and the eddy transports in setting large-scale property distributions in this region still remains to be estimated.

[4] The POMME experiment was designed to investigate the importance of mesoscales in subduction and biological processes. The data set collected is relevant for this investigation, as it provides circulation estimates and hydrological surveys resolving the mesoscales [*Assenbaum and Reverdin*, 2005] (hereinafter referred to as AR2005). The hydrological surveys are also spread over a time long enough (1 year) compared to the life cycle of most eddy structures, so that horizontal stirring caused by these mesoscales could be assessed. However, some (at least 3) coherent eddies were trapping water in their core for a multiseason period. In the case of the anticyclonic eddy A1, the retention time of the core even exceeded 1 year (J.-C. Gascard, personal communication, 2004). These cores could cover up to 5% of the domain area, and play a very specific role in eddy transport [*Le Cann et al.*, 2005].

[5] We will investigate the distribution of isopycnal properties of ENAMW in the four surveys. This includes potential temperature (T) (equivalently, salinity S), dissolved oxygen, and potential vorticity estimated as $q = f\,N^2/g$, where f is the Coriolis parameter, $N^2 = -g/\rho\, d\rho/dz$ is the Brünt-Vaïsala frequency and we have neglected relative vorticity which is usually small over most of the domain (alternatively, Brünt-Vaïsala frequency referred to as stratification is used). If vertical mixing (or radiative heating) plays little role on these distributions, T, S and potential vorticity are nearly conservative and characterize the water masses. Their evolution between surveys should be indicative of advection and horizontal mixing. Oxygen is not conservative, but adds an additional information as a clock (far from the surface, it should decrease in time as a result of remineralization and respiration processes). It is also revealing to plot oxygen saturation (the ratio of oxygen content to saturated oxygen), which should decay as water "ages" at subsurface. However, as the spatial variability in the isopycnal saturated oxygen (for example, 3 μmol/kg at σ_θ = 27.10) is less than the one in oxygen (10 μmol/kg), maps of oxygen content and oxygen saturation are very similar, and we will only discuss the oxygen content. The emphasis is on the upper layers that are directly ventilated at the surface in the intergyre region of the northeast Atlantic, in particular for sigma surfaces from σ_θ = 26.90–27.20 kg/m^3. The surface σ_θ = 27.10 kg/m^3 was near the minimum potential vorticity characteristic of ENAMW in the 1980s and 1990s. Stratification tended to be larger at densities higher than σ_θ = 27.15. However, denser layers with a very low stratification were occasionally found during POMME that will not be investigated in this paper: a particularly noticeable example being the core of eddy A1 that presents a low stratification at σ_θ = 27.18 kg/m^3 (J.-C. Gascard, personal communication, 2004). These layers are in the part of the θ-S diagram above the salinity minimum which separates them from the deeper water more strongly influenced by the Mediterranean water (MW) and to a lesser extent by Subarctic Intermediate Water (SAIW) from the northwest Atlantic (in the range $32.10 < \sigma_1 < 32.25$ and $\sigma_0 > 27.3$ [*Harvey and Arhan*, 1988]).

[6] The restratification happened relatively fast in 2001 (the bulk of the mixed layer retreat took place in less than a month according to *Lévy et al.* [2005] and *Paci et al.* [2005]), so that locally the core of low-stratification water should have been formed with a density close to the maximum surface one. Daily analyses of surface temperature (SST) data [*Caniaux et al.*, 2005] were used together with monthly analyses of sea surface salinity (G. Reverdin et al., Surface salinity in the Atlantic Ocean (30°S–50°N), submitted to *Progress in Oceanography*, 2005) to estimate the maximum surface water density reached over the POMME domain during the winter 2000–2001 (Figure 1). This shows that waters with a maximum density of 1027.10 (σ_θ = 27.10 kg/m^3) were ventilated during that winter within the POMME domain, whereas waters with larger density were ventilated farther north or northeast. The largest surface density of the domain was located in the northeast corner (near 45°N, 16°W), and the largest density in the northwest corner (reached at a later date than elsewhere in the domain) was on the order of σ_θ = 26.98 kg/m^3. The region with the lightest maximum surface density is near the southwest corner at σ_θ close to σ_θ = 26.70.

2. Data and Methods

[7] The hydrological CTD survey extends from 38°–45°N and from 15°20′W to 21°20′W during P1 (February 2001) and P2 (April 2001). The domain sampled is slightly smaller during P0 (October 2000) (north of 39°N) and P3 (September 2001) (39°–44.5°N). The station spacing is at best on the order of 55 km, and the hydrological surveys were done in roughly 20 days with one (P3) or two (P0, P1, P2) vessels, with only one of the vessels (R/V *Atalante* or *Thalassa*) reporting oxygen (the oxygen data are usually for the core of the domain). The station data we use are usually conductivity-temperature-depth (CTD) casts to at least 2000 m with some instances where the CTD cast was replaced by an XCTD drop, or when the CTD cast extends to the bottom.

[8] The accuracy of the salinity data has varied from cruise to cruise, as different institutions and instruments were involved, but is always at least at the 0.005 [PSS-78] level, and likely better than 0.003 or 0.004 [PSS-78] in most instances. The resulting uncertainty on temperature (salinity) on isopycnal surfaces is negligible compared to the

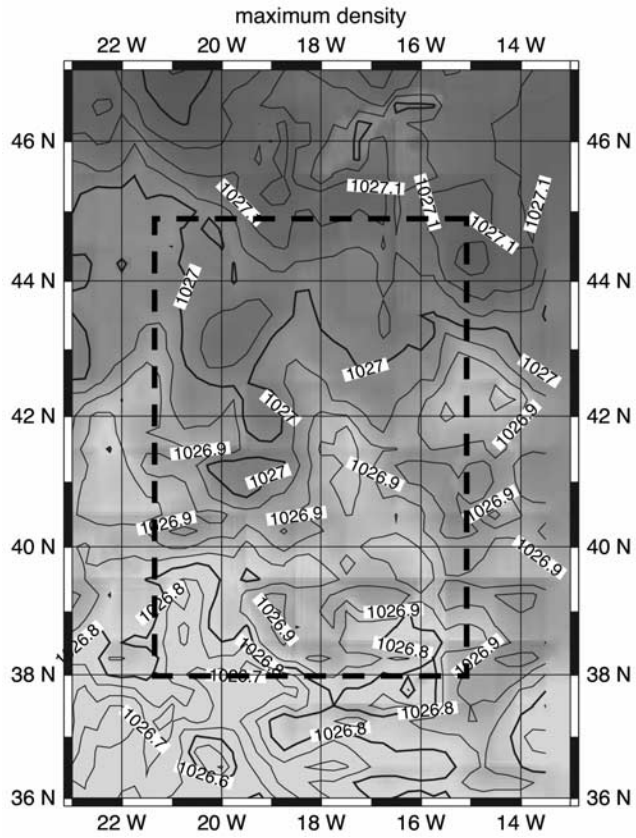

Figure 1. Maximum surface density during winter 2000–2001, estimated from the daily sea surface temperature (SST) data and the monthly surface salinity analyses. The Programme Océan Multidisciplinaire Méso Echelle (POMME) domain is surrounded by a dashed line.

variability observed. The oxygen data are from continuous profiles calibrated with samples collected during the upward cast. The accuracy of the calibrated oxygen data of the CTD casts is expected to be at the 2 μmol/kg level. There are small differences in deep water oxygen between P0 and the other cruises that might have resulted from systematic differences in the calibrations.

[9] Stratification ($N^2 = -g/\rho\ d\ \rho/dz$, the Brünt-Vaïsala profile, with ρ a locally defined potential density) is estimated from profiles smoothed over 10 db and taking differences over 25 db pressure intervals (the potential density is referred in these differences to the central depth). These N^2 estimates have very skewed distributions, and extreme high values are removed (with a threshold at 30 10^{-6} s^{-2}) in order to reduce noise in the statistical estimates (mapping assumes that the distribution is Gaussian, which is far from realized). To check the N^2 maps, we also used the distance between two ispoycnals, which is more Gaussian distributed, and should be proportional to $1/N^2$. Usually, N^2 is weakest for 27.15, but occasionally weakest at 27.10 (for example during P0 at 39°N or 44°N), or even at 27.18 or up to 26.95 in individual profiles. The waters above 26.95 or below 27.20 are usually more stratified.

[10] Data are then extracted from the continuous profiles on sigma (potential density) surfaces with a step of 0.05 kg m^{-3}, both for a reference at the surface or a reference at 1000 db. We do not retain data whose density is within 0.02 kg/m^3 from the surface density or within 25 m of the sea surface to avoid a too large influence of the surface layer. The analyses with the two reference levels for density are very close, indicating an insignificant importance of deviations of the isopycnal surfaces from real neutral surface. We will only present the one with the surface reference.

[11] Mapping by an objective analysis method is then performed [*Bretherton et al.*, 1976]. Data from the surveys plotted on sigma surfaces present a complicated pattern with obvious influence of mesoscales, but with a usually striking north-south structure. For this reason, we approached the analysis by first estimating meridional profiles of zonal averages of the properties on the sigma surfaces, and then analyzing by objective mapping the residual from these averaged profiles. These residual are then combined with the average profile to produce the mapped field. We performed usually two analyses, one in which the data are positioned where the stations were collected, and one in which the positions of the data have been moved by advecting them by the currents of weekly analyses (AR2005) to estimate locations at a common date (near the middle of the cruise). The currents correspond to the depth of the data (estimated by linear interpolation between the analysis at 100 m and 400 m), and are kept constant through the advection. This second set of analyses was done to get a sense of the error resulting from the nonsynopticity of the CTD array (the CTD casts of one array were collected over more than 20 days).

[12] The two analyses result in close-by zonally averaged distributions, but the mesoscale features portrayed on the maps can be rather different (example in Appendix A). In addition, it is clear that the array resolved marginally the mesoscales, with many features tracked only by one station, but often corresponding to known circulation features (based on the larger set of data that can be used to estimate the currents (AR2005)). The mapping used fairly small correlation scales (typically comparable to the station spacing), so that it does very little averaging of the structures, but the result is that mesoscale features might be strongly aliased by the mapping.

[13] The depths of the different isopycnal surfaces are also mapped and are strongly influenced (even for the zonal averages) by the mesoscale circulation. The average depths are on the order of 450 m for the $\sigma_\theta = 27.15$ surface, 300 m for $\sigma_\theta = 27.05$, 200 m for $\sigma_\theta = 26.95$ and 100 m for 26.80, and present typically a 100 m range in the POMME domain. These surfaces present a jump (deeper to the south) centered between 41° and 42°N during P1 and P2, but less so or at other latitudes during P0 and P3, and will not be discussed further in this paper. The surfaces lighter than $\sigma_\theta = 27.10$ reach the mixed layer during winter in parts of the domain, first in the northeast, but for the lightest sigma surface ($\sigma_\theta = 26.90$) as far south as 41°N.

[14] Finally, to understand better the evolution of the mapped distributions on isopycnal surfaces, we carry on quasi-Lagrangian diagnostics. This is done by seeding selected parts of the maps as sources of trajectories estimated with the weekly stream function analyses (AR2005). Because these analyses are derived from a stream function,

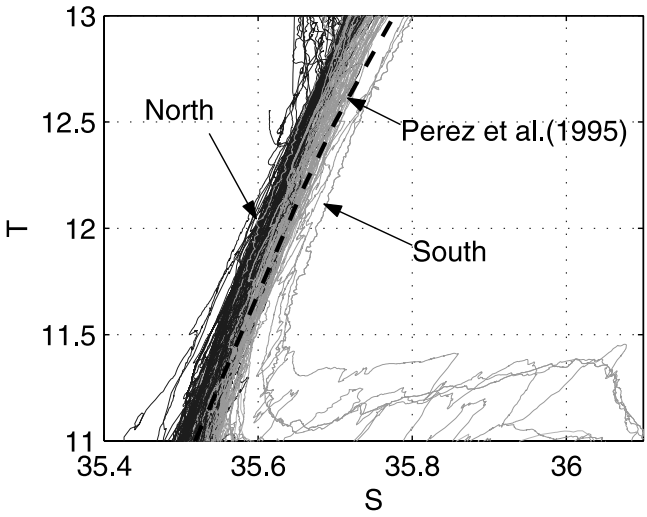

Figure 2. Average *T-S* relationship (*T* is potential temperature) for the POMME survey P1. The dark (light) lines are for individual profiles north (south) of 41.5°N. The dashed line represents the climatological *T-S* relationship for Eastern North Atlantic Mode Waters (ENAMW) adopted by *Perez et al.* [1995].

the density of the horizontal trajectories is a conservative quantity. We compared this approach with one based on tracer advection with very similar results. Dispersion in the trajectories occurs as a result of the small scales in the currents, but also as a result of the changes from week to week (for instance, simulated trajectories do not remain trapped in eddy cores). Nonetheless, the dispersion statistics of the stream function analyses are at first glance rather comparable to the observed ones, and we do not introduce an explicit diffusion operator. For that reason, the diagnostics can be carried either forward or backward in time.

3. Large Scales

3.1. Meridional Structure

[15] The *T-S* diagrams in the ENAMW range present a tendency to be shifted to the right of the diagram in the southern part of the domain compared to the northern part (warmer and saltier on isopycnal surfaces) (Figure 2). The slope of the *T-S* distribution is also steeper than the reference curve for the northeastern part of the domain presented by *Perez et al.* [1995]. For the lighter sigma surfaces, this implies noticeably cooler and fresher waters than for this reference based on data from the 1960s and 1970s. There is also a smaller east-west average gradient in *T-S* properties at least north of 41°N. This dominance of the meridional gradient over the zonal gradient is also found for oxygen and less consistently for stratification.

[16] These gradients are illustrated by the profiles of the zonally averaged data for two surfaces (Figure 3) rather typical of the other surfaces in the ENAMW layer. The region where the meridional isopycnal temperature gradient (or salinity, not shown, but with roughly 0.05 [PSS-78] change in *S* for 0.2°C change in *T*) is most pronounced, varies between surveys and surfaces. It is most intense and near 39°–41°N during P0, spreads between 38°N and 42°N during P1, and between 38°N and 41°N during P2 (with lower temperatures). It is more regular during P3, when it is rather weak at σ_θ = 26.95 and shallower surfaces (with

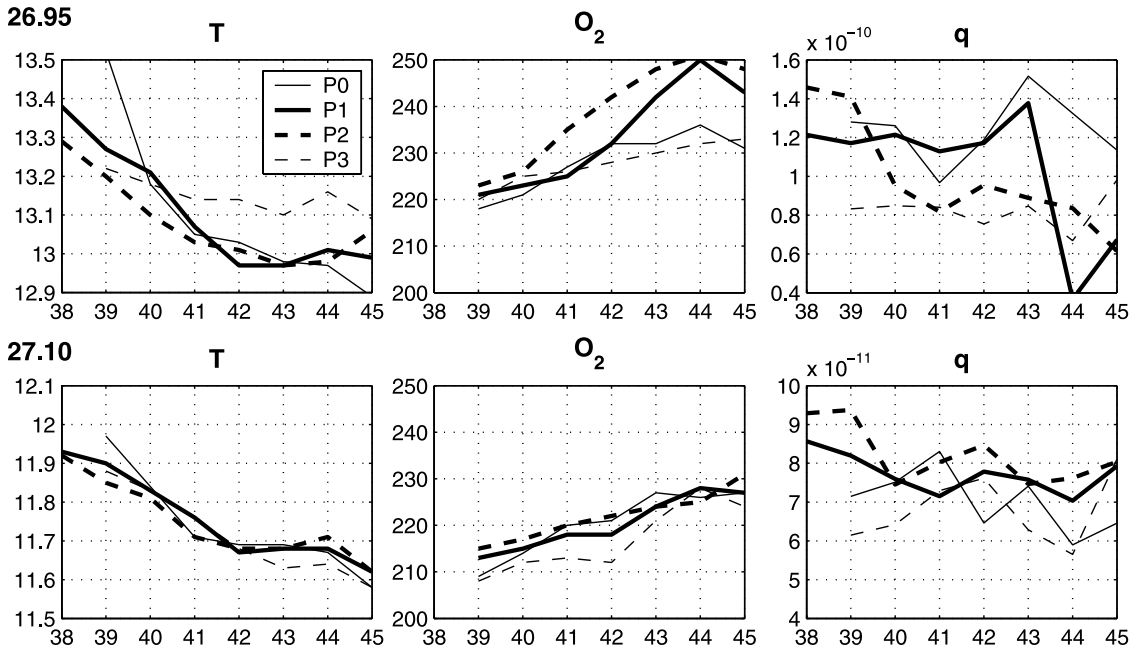

Figure 3. Zonally averaged distributions of (left) *T*, (center) O_2, and (right) *q* for two isopycnal surfaces. On each surface the four curves correspond to the cruises P0, P1, P2, and P3. Notice that there is no oxygen data south of 39°N and no data south of 39°N during P0 and P3 and that there are very few stations at 44°–45°N on σ_Θ = 26.95.

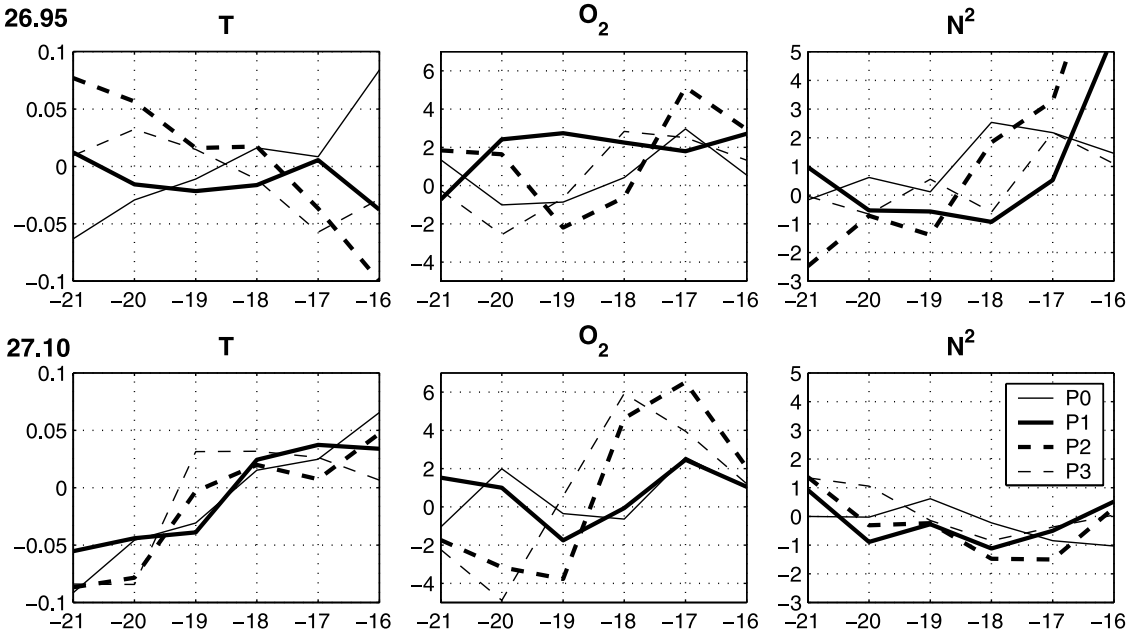

Figure 4. Meridionally averaged distributions of (left) T, (center) O_2, and (right) N^2 (multiplied by 10^6 m s^{-1}) deviations from the averages in Figure 3 for two isopycnal surfaces (only stations north of 41.5°N are retained). On each surface the four curves correspond to the cruises P0, P1, P2, and P3.

warmer temperatures). During all surveys, there seems also to be a temperature gradient in the deep surfaces near 44°–45°N.

[17] During all surveys dissolved oxygen content (or oxygen saturation) presents a rather more homogeneous decrease from north to south (between 44°N and 39°N, the common area sampled by the cruises) than temperature (salinity) (Figure 3). There is also a tendency for oxygen on surfaces at or above σ_θ = 27.05 to have smaller values during P0 and P3 (late summer) than during P1 and even more P2, at least north of 41°N. This is typical of what one expects of oxygen consumption by respiration and remineralization at these depths during and after the spring bloom. On the deeper sigma surfaces (for example, σ_θ = 27.10), however, oxygen presents larger values during P0 than during later surveys north of 41°N, whereas P3 presents lesser values everywhere. The oxygen content is also usually a little larger during P2 than during P1 south of 42°N. This together with the lower temperatures would suggest a southward displacement of the water masses during the two surveys (by roughly 1°). However, quasi-Lagrangian statistics presented by AR2005 indicate that there was little input of water from north of 42°N to these southern regions from P1 to P3. They suggested that flow to the south clearly identified in the southern part of the domain was compensated by inflow from the west in the eastward current often found near 41°–42°N. What actually happened will have to be investigated in more details when investigating the property distributions during the surveys.

[18] For σ_θ = 26.95 during P1 and P2, the oxygen saturation typically varies from 88% at 39°N to 98% at 44°N (this surface has been ventilated in those areas during the winter), whereas for σ_θ = 27.10, it varies from 82% at 39°N to 87% at 44°N, so that even though 44°N is relatively close to areas with direct ventilation (starting at 46°N), only a small percentage of the water at that latitude has been directly renewed by newly ventilated waters. This will also have to be investigated in more details from the maps during the individual surveys.

[19] Potential vorticity on the deep sigma surfaces (σ_θ = 27.10 (Figure 3)) presents a slight gradient toward increasing values in the south, at least south of 41°N for P1 and 40°N for P2. There is no clear gradient for P3 (notice that the estimates are rather uncertain, due to noise in the estimates that are medians of a highly non-Gaussian distribution). At shallower surfaces (σ_θ = 26.95), and notwithstanding the values of P1 at 44°N and 45°N based on very few profiles, there is a striking change between P0, P1, on one hand, and P2 (north of 40°N) or P3 which have much lower values. This, together with the higher oxygen during P2, suggests the local formation in early 2001 of a water that was not present in early 2000 (this was checked from a POMMIER2 survey in April 2000 in the same region). However, the low oxygen during P3, and the fact that the temperature is higher during P3 raise some questions on this local interpretation. Experiments presented by AR2005 show a high degree of particle exchanges with neighboring regions (in particular zonally) between February and October 2001. There is therefore little reason for expecting a continuity of the evolution between P2 and P3, and the differences could reflect differences in water mass properties with neighboring regions.

3.2. Zonal Structure

[20] Overlaid to this meridional structure, there is a weaker zonal one, at least north of 41.5°N illustrated on two isopycnal surfaces (Figure 4, after removing at each latitude the zonal mean presented in Figure 3). The gradients are most consistent in time for the deeper isopycnals (σ_Θ = 27.10), and fit there with the expectation from the study of *Perez et al.*

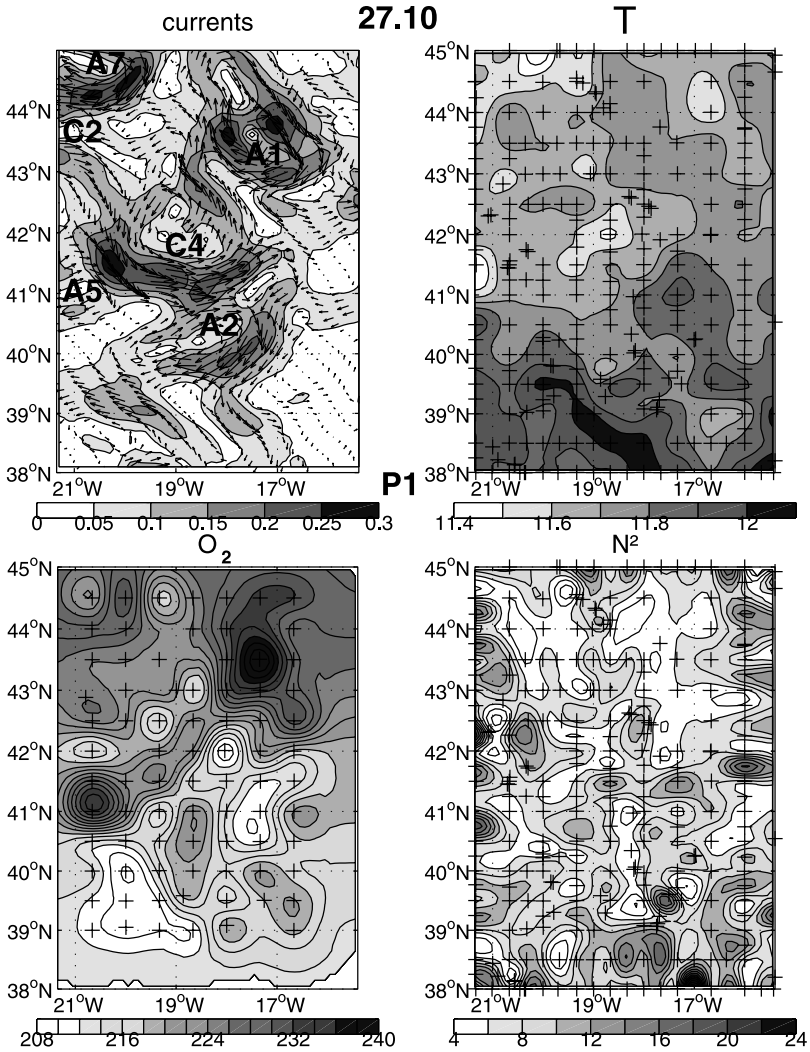

Figure 5. Properties on σ_Θ = 27.10 during P1. (top left) Currents at 100 db, with a few names of structures (A for anticyclones, C for cyclones). (top right) *T*, (bottom left) O_2, and (bottom right) N^2 on this surface, with crosses indicating data positions.

[1995] or even, but less clearly in *van Aken* [2001] of increasing *T* (and *S*) eastward toward the Iberian peninsula (0.1°C corresponds to 0.025 [PSS-78]). Interestingly, on σ_Θ = 27.10, low-*T* water in the west are not associated with higher oxygen or lower potential vorticity contrary to the meridional profile. There are large differences in oxygen from cruise to cruise with a large change between P1 and P2 (P0 and P1 on one hand and P2 and P3 are rather similar) with a fairly large increase between 18.5°W and 16°W, and a decrease farther west. This high-oxygen water is also associated with lower stratification. This is suggestive of the arrival of a recently ventilated water to this region starting during P2. This will have to be investigated carefully from the regional surveys and quasi-Lagrangian diagnostics.

[21] On the shallower surface (σ_Θ = 26.95), there is again a similarity between P2 and P3, and a big departure from the earlier surveys. These illustrate a warmer water during P2 and P3 in the west (and fresher in the east), seemingly associated with lower stratification, but not clearly with higher oxygen. This might relate to differences in the local conditions of formation of these lighter waters in the northern part of this domain, and the changes between P1 and P2 will need to be investigated further in the regional surveys. As was stated earlier from the meridional profiles, it will be however difficult to extend the conclusions to P3.

4. Isopycnal Distributions

[22] The focus of this section will be in the mesoscale property fields. In particular, we want to illustrate qualitatively how they are linked to specific circulation features and the role of spring restratification in setting them. First, we will comment on the surveys for P1 (3–24 February 2001) and P2 (22 March–13 April 2001) that happen just before and just after the major spring retratification episode [*Paci et al.*, 2005]. These are the most complete surveys with the best hydrological coverage of the POMME region. Then we will present the late summer survey P3 (23 August–13 September 2001) and for reference the earlier late summer survey P0 (18 September–12 October 2000).

4.1. P1 Survey (3–24 February 2001)

[23] Temperature gradients can be quite large on sigma surfaces (Figure 5) and are located somewhat to the south of

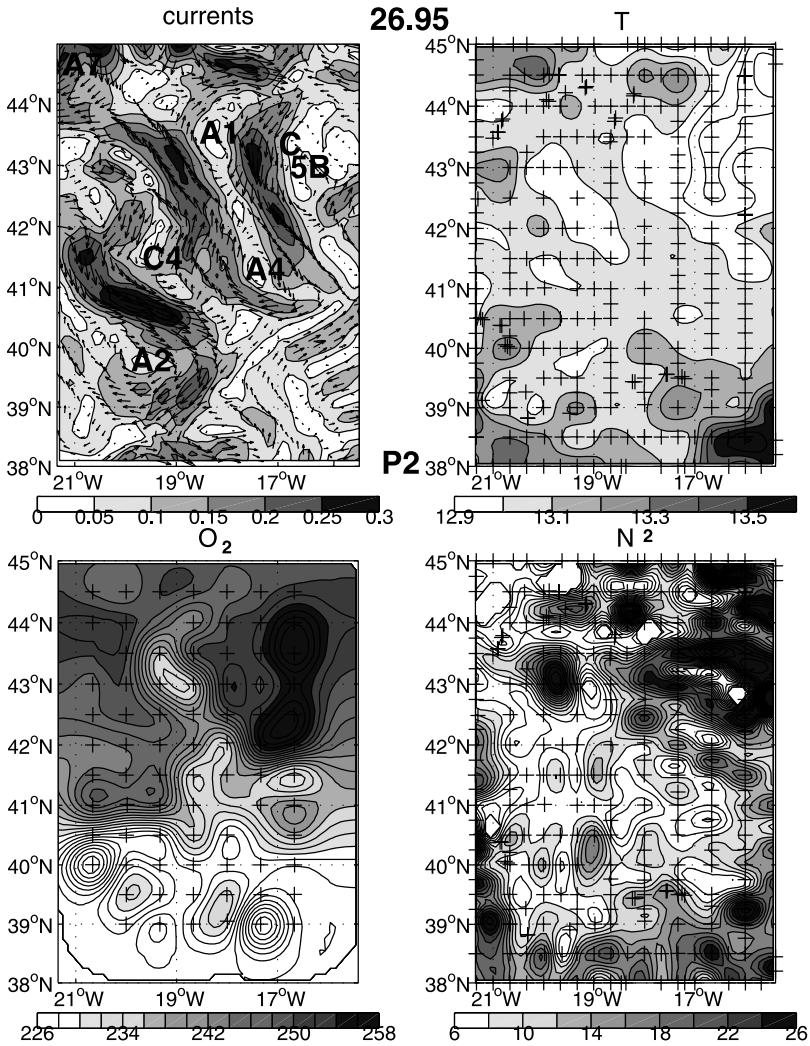

Figure 6. Same as Figure 5, but for P2 (σ_Θ = 26.95).

the eastward current located near 41°–42°N. The southwest region presents high isopycnal temperature, low-oxygen water, with a tendency for the highest-*T* water to be aligned in an anticyclonic ridge to the east of the lowest-oxygen water. The water with low *T* on σ_Θ = 27.00–27.15 (Figure 5) is found in the northwest region (north of 44°N, 19°–21°W) and is associated with the elongated anticyclonic eddy A7. A7 was a major feature from P1 to almost P3 with a western part that reinforced between P1 and P2 compared to its eastern part without moving much. Floats (and trajectories) suggest that part of this low-*T* water may be trapped within the eddy and is reminiscent of water with ''western'' characteristics. This eddy core also got a very deep winter mixed layer (on the order of 400 m with a density σ_Θ = 26.95) that remained unstratified later than elsewhere to at least the middle of the P2 survey.

[24] Below σ_Θ = 27.05, dissolved oxygen is rather patchy with various high-oxygen cores. There is an isolated maximum near 41°–41.5°N, 21°W with no particular *T* or stratification signal associated (Figure 5) just to the east of anticyclone A5. This structure is deep-reaching with evidence of Mediterranean water in its core structure and has drifted from a position near 43.5°N, 19.5°W during P0 [*Le Cann et al.*, 2005]. Two stations during P0 on the rim of A5 also showed high dissolved oxygen, suggesting an advective origin of the feature. However, both P0 and P1 surveys have insufficient coverage to be fully conclusive.

[25] The area with highest dissolved oxygen is found in the northeast between 43°N and 44°N associated with a southward current (the southward extension of the high O_2 corresponds to the transition to warmer temperatures), but on some surfaces also with the eastern portion of anticyclonic eddy A1. The southward current to the east of A1 does not present a signature in temperature, and its minimum stratification is found on σ_Θ = 27.10. On σ_Θ = 27.10, this stratification is lower there than elsewhere during P1 as well as compared to what was found during P0 in the area. An hypothesis would be that this subsurface water has been renewed at the surface in early 2001. The closest source compatible with the currents is near 45°N, 17°W where σ_Θ = 27.10 could have surfaced by 24 January, more than 2 weeks before the survey. Such an advection is not likely with the observed currents at these depths, although it cant be ruled out and becomes more likely on lighter sigma surfaces. The other hypothesis would be advection without ventilation from regions with higher oxygen. Such high

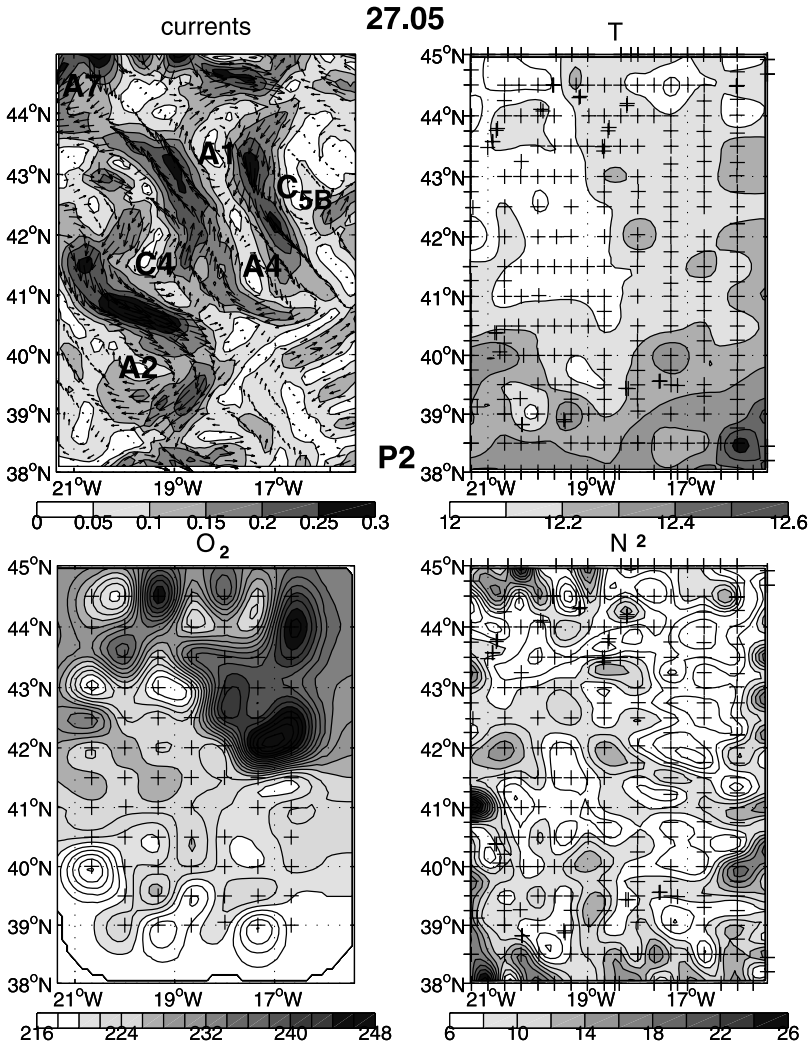

Figure 7. Same as Figure 5, but for P2 (σ_Θ = 27.05).

oxygen were not measured during the P0 surveys within the POMME domain, but are still within the realm of what could be observed possibly a little farther north.

[26] Within C4, there is a rather homogeneous pool with a fairly low T (Figure 5 for σ_Θ = 27.10). Float trajectories suggest that this core of water stayed in this region for a large part of the life of C4. There is more contrast toward the eastern or southern sides of C4 on the deep surfaces (above and below σ_Θ = 27.00 during P1, the surfaces in C4 are close to the mixed layer). In particular, to its east near 17.5°W south of 42°N, there is a region of fairly high *T*, low dissolved oxygen bulging to the north that seems to follow the contour of the rim current of C4 (this appears as a tongue of unventilated water on shallower surfaces as σ_Θ = 26.95 that gets entrained northward by the current, and is also seen in the surface layer as a tongue of warm, salty water).

4.2. P2 Survey (22 March–13 April 2001)

[27] This survey presents major spatial contrasts in *T*, O_2 or stratification clearly related to the circulation or to newly restratified water. On shallow surfaces (σ_Θ = 26.85–27.00) (Figure 6), there is a clear cold and oxygen-rich signature along 19°–20°W north of 40.5°N which follows the southward current on the western side of cyclone C4. Simulated trajectories (not shown) indicate that this water originates during P1 mostly to the north of this cyclonic region (44°N, 18–20°W), a region that has denser surface water. This is clearly newly ventilated water, with perhaps a contribution of primary production to the high oxygen which was observed to be taking place during survey P2 on these shallow surfaces (often within 100 m of the surface).

[28] To the west of this tongue, along the eastern rim of the cyclonic region C4 along 18°–19°W, there is a region of warmer water (at least noticeable down to σ_Θ = 27.00) that is associated with lower dissolved oxygen that seems to extend northward at least to 44°N (Figure 6). This region corresponds to the northward current (or slightly to its east) that is defining the eastern rim of cyclone C4. This suggests a fairly southern origin to this water mass. This low-oxygen, high-*T* water was also found during P1, but extending only to 42.5°N (farther north σ_Θ = 26.95 reached the surface). Its extension to the north is compatible with the circulation and correspond to a path taken by floats in March 2001.

[29] Similarly to what was found during P1, cold (above or at σ_Θ = 27.00) and oxygenated (all surfaces) water is

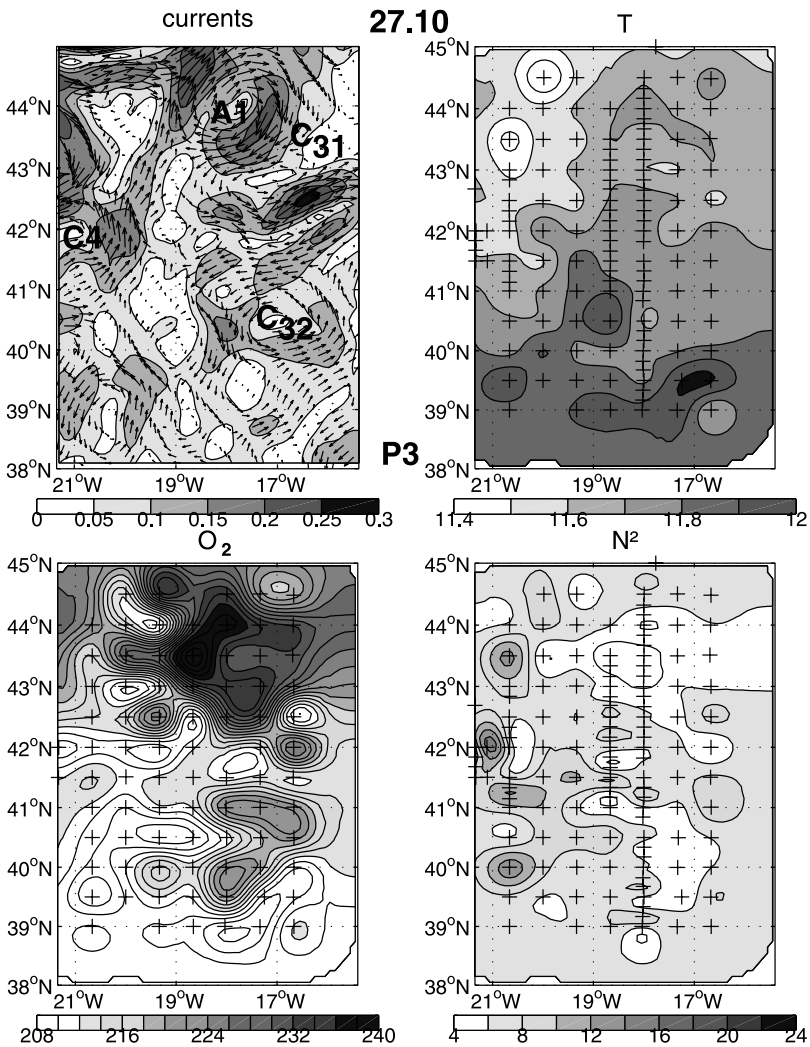

Figure 8. Same as Figure 5, but for P3 (σ_Θ = 27.10). Note that there were no O_2 data south of 39°N.

found farther east (16°–17°W, north of 42°N). The core of this water is within a cyclonic region (C5) to the east of anticyclone A1. It is slightly to the east of an intense southward current, with a circulation that is weak but mostly to the south according to the reanalyses. The very low *T* in that tongue on σ_Θ = 26.95 is rather remarkable and is responsible for the change in large-scale zonal gradients with the previous surveys (in particular P0). There are already indications during P1 that in this northeast corner, the newly formed water with σ_Θ = 26.95 would be fresher and colder. However, this is highly stratified water (the winter surface mixed layer is much denser there, and the core of formed water during spring mixed layer retreat is denser) and this would correspond to a much weaker volume of water formed that in the northwestern corner. The shape of the high-oxygen region is rather different on different surfaces (notice that we do not know the eastward extent, as the oxygen survey stopped at 16°W). It is elongated on σ_Θ = 26.95 corresponding roughly to the very cold *T* water (Figure 6), extends farther west (including A1) on σ_Θ = 27.00 (not shown), whereas on σ_Θ = 27.05 (Figure 7), the core corresponds to a low stratification with a similar spatial distribution. For the southern part of this oxygen maximum (near 42°N), σ_Θ = 27.05 is also the surface with minimum stratification in the vertical. This is suggestive of a recently ventilated mode water. This surface was ventilated through the winter and until late March in fairly deep mixed layers near or north of 44°N, that could have resulted in a mode water advected with the currents. This contrasts with P1, where the similarity between oxygen and N^2 distributions was found mostly for the deeper σ_Θ = 27.10 (or 27.15) surface that may not have been ventilated in the same year, or farther north.

[30] There are also (3) isolated points (one station each) with low dissolved oxygen in the southern portion of the domain that are found on most surfaces (Figures 6 and 7). The temperature analysis suggests that this usually coincides with local maxima in temperature, although not always with a similar amplitude, and therefore could be remnants of the high-*T*, low-oxygen water found during P1.

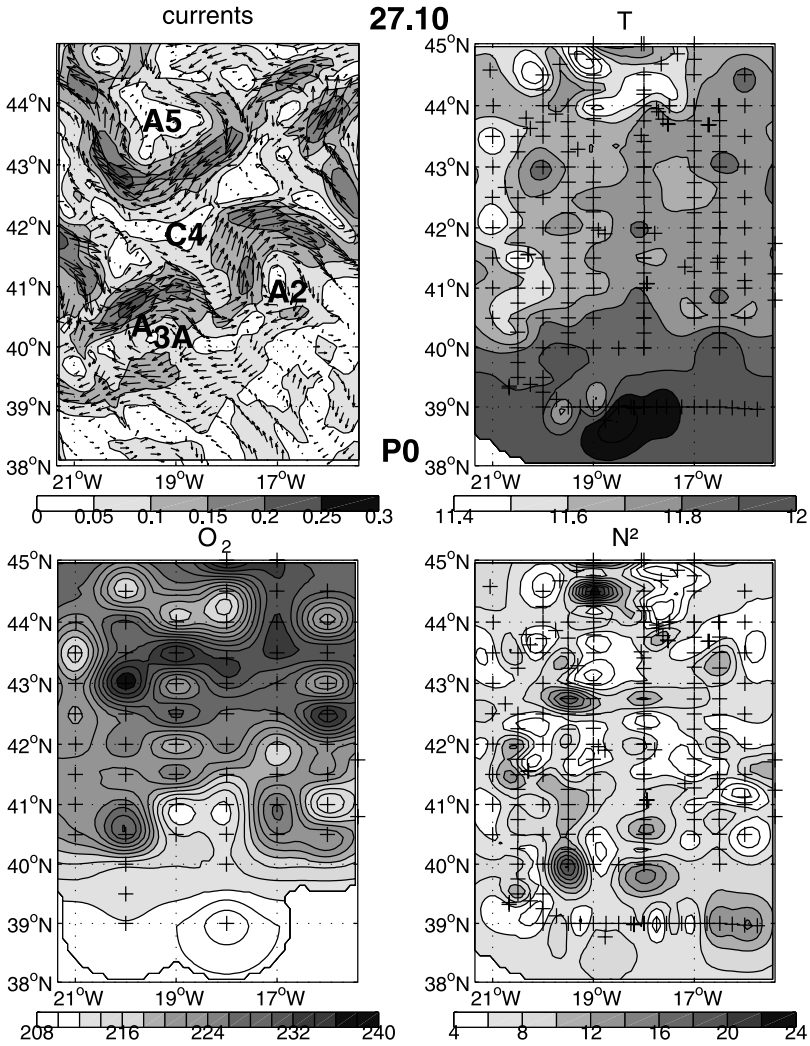

Figure 9. Same as Figure 5, but for P0 (σ_Θ = 27.10). Note that there were no O_2 data south of 39°N.

The survey does not have the proper resolution to fully identify the mesoscale structures to which they are associated. Also, oxygen might be a less reliable tracer of circulation during P2 than T on isopycnal surfaces: production has been ongoing for a while in this region [*Fernández et al.*, 2005] and there might already be some effect of remineralization or respiration on the oxygen distribution.

4.3. Late Summer Surveys (P3 23 August–13 September 2001 and P0 18 September–12 October 2000)

[31] During P3 (Figure 8), the zonal T gradient near 18°–20°W north of 40°N is to the east of a northwestward flowing current with some anticyclonic features to its east. The correspondence between T and O_2 or stratification is somewhat muddled. In the same latitude band, there is a tendency however for the cold/fresh waters to be stratified and less oxygenated, although the correspondence is not that good for oxygen. This contrasts with the meridional gradient associating warmer/saltier and lesser oxygen in the south compared to the north. Surprisingly, low stratified waters are found all the way to 39°N, in regions that have rather warm waters and are not that oxygenated. Except for this apparent anomaly near 39°N, there is a tendency for areas of weak stratification to match those of high oxygen (σ_Θ = 27.10 in Figure 8). There is also a tendency that areas with comparably low stratification have higher dissolved oxygen in the north than in the south. The southern region with low stratification/high oxygen in the southeast (39.5°–41°N) corresponds to a cyclonic region (C_{32}) and an extension to its south. These oxygen contents are larger than 150 days earlier during P2.

[32] During P3, the southeastern cyclonic region C_{32} is separated by an area with lower oxygen and higher stratification (also higher T on some upper surfaces) from a region with low stratification/high dissolved oxygen farther north (42.5°–44°N). This latter region corresponds both to a region with cyclonic circulation C_{31} and to the anticyclonic eddy A1. Whereas low stratification is often associated with high oxygen on the deep surfaces, the surfaces shallower than σ_Θ = 27.00 present no such relationship during P3 (not shown). Those relatively shallow horizons were probably

influenced by seasonal warming due to penetrating solar radiation or by vertical mixing in the seasonal thermocline. Oxygen changes due to biological activity will also have taken place.

[33] During P0, the mesoscale distribution of isopycnal temperature does not always exhibit a clear relation with the circulation. However, the colder (fresher) band near 21°W north of 40°N seen on most surfaces (σ_Θ = 27.10 in Figure 9) corresponds to a southward current vein connecting the northern part of the domain to 40.5°N that transported one float (north of 42°N, this current is just to the west of the survey). Interestingly, although coming from the north, this water is associated with fairly low oxygen content on σ_θ = 27.05 and deeper surfaces. There is water with comparable low T and O_2 in the central and western part of the domain north of 44°N which might have the same origin. There is warmer and more oxygenated water to their east and southeast in particular associated with the circulation around the anticyclone A5. As during P3, these associations at the mesoscale contrast with the large-scale meridional gradients, which associate low oxygen (near 80% saturation on σ_Θ = 27.10 in the south) with warm/salty water on isopycnal surfaces. There is only a weak correspondence between the mapped oxygen and stratification taken in a similar latitude range (high O_2 and low N^2), although the fields (in particular O_2) are insufficiently sampled and the N^2 data are very noisy (slightly better correspondence with isopycnal separation, not shown). These fields and the association with the currents suggest that on these isopycnals there is a source of warmer (saltier), more oxygenated, and maybe less stratified waters to the northeast of the domain than to the northwest (this is consistent with inferences from the Vivaldi 1991 survey [*Pollard et al.*, 1996]).

5. Discussion

5.1. Large-Scale Fields

[34] The northern part of the POMME domain corresponds to the southern limit of the formation region of ENAMW. We found a tendency in the northern part of the domain for the *T-S* relationship to be rather shifted to the left of reference *T-S* curves [*Paillet and Mercier*, 1997; *Perez et al.*, 1995] (the relationship shown in Figure 2), a tendency which is less present in late summer 2001 than in the late summer 2000 on the sigma surfaces lighter than σ_Θ = 27.00. This means colder and fresher waters on isopycnals than in earlier surveys from the 1960s or 1970s north of 41°N. Differences in mode water properties are expected close to the formation regions, as there is a large year to year variability in the mode water (ENAMW) characteristics, as well as in their distribution and region of formation, as seen for example in high-resolution model simulations [*Valdivieso da Costa et al.*, 2005] or in some data sets [*Pollard and Pu*, 1985; *Perez et al.*, 1995; *Pollard et al.*, 1996]. As the new water is in contact with the atmosphere or is within the euphotic zone, it resets its oxygen to near saturation levels. This creates a north-south contrast in properties between the newly formed water to the north and the "older" waters to the south. *van Aken* [2001] indicated the presence of a meridional isopycnal gradient in oxygen even without one in temperature (salinity). The oxygen gradient was then interpreted to result from oxygen utilization by respiration and degradation of organic matter as the central waters advect southward.

[35] During the POMME surveys, however we find an average meridional gradient in T (S) south of 42°N not found in the work of *van Aken* [2001]. The analysis of the mesoscale circulation (AR2005) indicated that the average meridional velocity in these layers near or north of 42°N is much weaker during POMME than the 1 cm/s value retained by *van Aken* [2001], which is also the order of magnitude found in the inverse model of *Paillet and Mercier* [1997]. This puts somewhat in question the renewal by an average advection from the north of the waters in the south during the POMME surveys. Interestingly, there is a similarity between the large-scale circulation and the gradients of properties. For P1 for example, the largest temperature gradients are located near a ridge of anticyclonic structures. This ridge has been present during a large part of the POMME year, and remains a major surface reinforced structure in the annual averaged circulation (AR2005). From the altimetric maps, the eastward current to its north seems to be part of an anomalous current vein extending from west of the Mid-Atlantic Ridge to the vicinity of Portugal. Trajectory experiments indicate that very little of the water south of the ridge originates from north of the eastward current. It played a role in partially isolating the southern part of the domain from an influence of the more northern mode waters (at least from the summer 2000 to the late winter 2001).

5.2. Mesoscales

[36] Nonetheless, the changes witnessed on sigma surfaces in the south from P1 to P2, and to P3 are strong. In particular, the dissolved oxygen increase between the winter to the early spring, which continues to the autumn south of 41°N (Figure 3) points out that the subsurface layers in the southern part of the domain are somewhat renewed by more oxygenated waters (the seasonal change is also present in macronutrients [*Fernández et al.*, 2005]). We tested this evolution with simulated trajectories focusing on areas with particular T or oxygen noted in section 4.

[37] One such case is the region with relatively fresh and oxygenated water present during P1 to the east or north of A2 in this southern domain. Backward trajectories from P1 indicate that this water largely entered the POMME domain from the west in the eastward current near 41°–42°N. These and trajectory experiments for other areas all suggest that the eastward current has been a source of renewal of the "older" mode waters in the southern part of the domain in 2001. Forward trajectories illustrate the spreading of the oxygenated water between P1 and P2 in the southern part of the domain, mostly to the southwest where they displaced the warmer and oxygen-poor water (Figure 10a). The forward trajectories simulations suggest that a large portion of this water reaches during P2 the area near 39.5°N, 20°W or a little farther west near 20.5°–21°W. On σ_Θ = 26.90, the analyzed T, O_2, N^2 at the end of the trajectories were (averaged value followed by RMS scatter in parenthesis) 13.49 (0.08), 238 (6.5) and 12.9 (9.3), very close to their values at the beginning of the trajectories 13.44 (0.03), 235 (5.6), 11.4 (4.4), whereas the values at the end positions, but for the P1 survey were 13.72 (0.20), 224 (9.7), 18.7 (8.1).

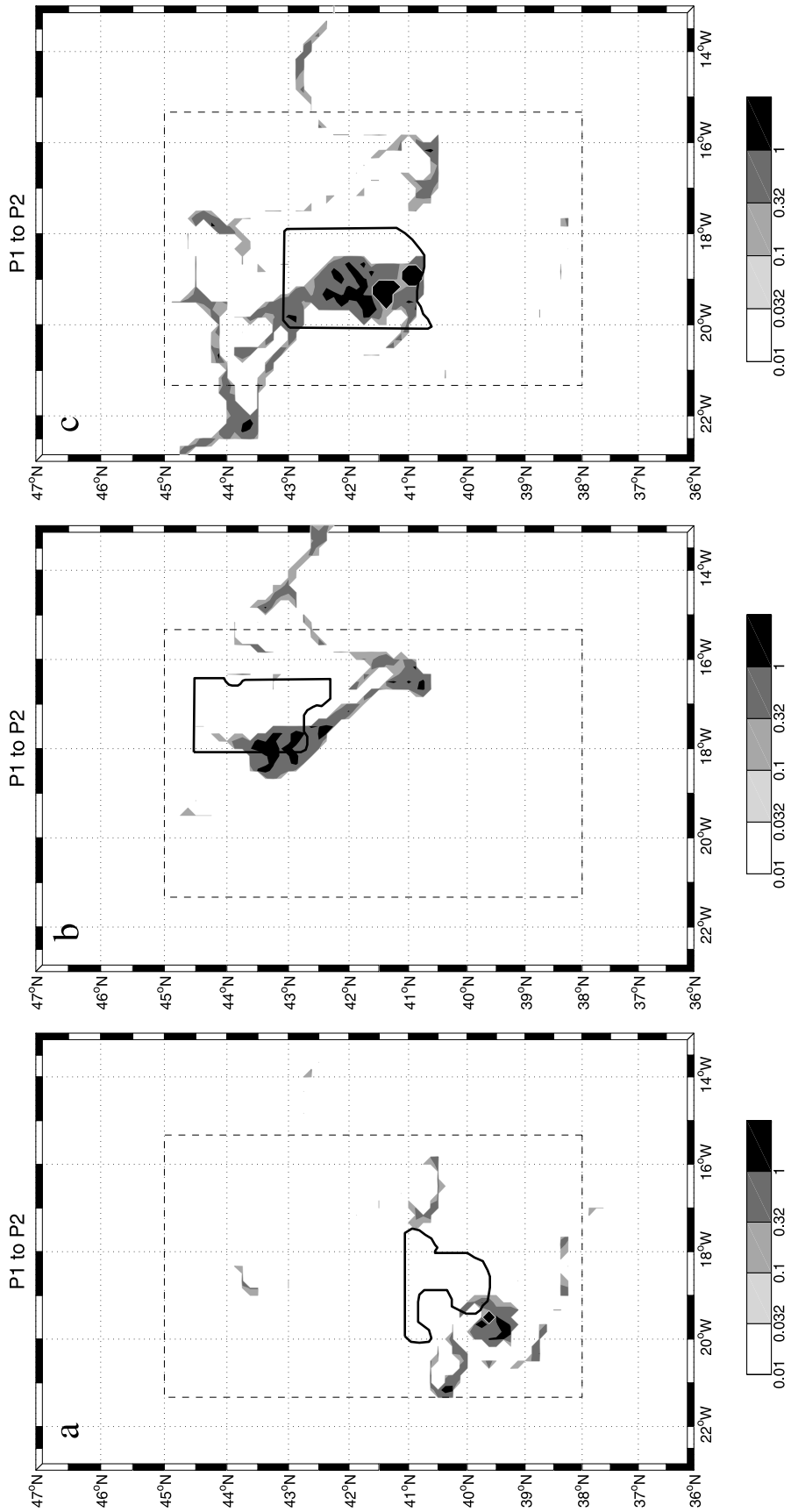

Figure 10. Forward quasi-Lagrangian experiments from a region surrounded by a bold line during one survey to the next survey. The density of end points of the trajectories is plotted (the value 1 corresponds to the density equivalent to the one in the selected origin region, and isolated dots correspond to single trajectories). (a) P1 (region surrounded by a bold line where cooler, oxygen-rich water was found) to P2. No trajectories crossed the boundaries of the analysis domain (note that it is larger than the POMME domain surrounded by a dashed line). (b) Forward trajectories from P1 (region with oxygen-rich water on σ_Θ = 27.10) to P2 (15.4% of the trajectories crossed the boundaries (mostly eastern) of the analysis domain). (c) Forward trajectories from P1 (extended C4 domain) to P2 (1.4% of the trajectories crossed the boundaries (mostly eastern) of the plotted domain).

This similarity in the average values and in the standard deviations along the trajectories between P1 and P2 reinforces the scenario of isopycnal replacement of the water in the southwest part of the POMME domain between these two cruises. We expected however a decrease in dissolved oxygen related to the large bacterial production and remineralization found at subsurface in this area (σ_Θ = 26.90 is near 250 m depth) [*Maixandeau et al.*, 2005].

[38] Large changes were observed between P1 and P2 in the northern part of the domain during this period of mode water formation. We discussed the arrival during P2 of a newly formed mode water at σ_Θ = 27.05 in the northeast advected by a southward current. However, what became of the previous denser mode water at σ_Θ = 27.10 during P1? On the basis of forward trajectories from P1 to P2 (Figure 10b), part of the water with high oxygen remains trapped in A1 as it moves westward between the two surveys, whereas part of it (in the southward current east of A1) was spread as a long and inhomogeneous filament to 12°W following the current that reached 41°N near 17°W and then meandered northward and eastward. This current vein has been observed and has been followed by a large number of surface or near-surface drifters and floats. As close to 75% of the trajectories remain in the domain, a more quantitative assessment can be made. The displacements suggested by the simulated trajectories are coherent with the small changes in T and O_2 (on σ_Θ = 27.10) between P1 and P2 following the simulated trajectories (11.70–11.72 and 233–230 in T and O_2 with rather comparable dispersion). The changes witnessed at the end positions of the trajectories between P1 and P2 are also small (11.73–11.72 and 224–230) but with more scatter during P1.

[39] The center of the POMME domain is characterized by the large cyclonic feature C4 which presents a rather homogeneous core surrounded by property tongues on its sides. Forward trajectories (Figure 10c) show that it trapped a large proportion of its water between P1 and P2 as it shifted to the west, but suggest some loss of water from C4 to its north with trajectories then veering westward and ending near 43°–44°N in the northwest, south of anticyclone A7. The low scatter in T or O_2 in this region during P1 is kept at the end positions of the trajectories during P2, reinforcing this scenario of advection. It was not a region of particularly large mode water formation [*Paci et al.*, 2005].

5.3. Eddy Transport

[40] From the previous examples, we expect that the transports by the mesoscales will contribute to the changes in the property distribution, in particular after restratification. It would therefore be interesting to derive the meridional (or zonal) profiles of second-order moments (eddy transport terms). These transports are estimated from the mapped properties with the analyzed mapped currents of AR2005 (for example, for meridional transports, at each latitude a zonal average is removed and a zonally averaged eddy transport is estimated). This is however a very noisy estimate, even after averaging the estimates at the different latitudes (narrow domain), and in particular for oxygen or potential vorticity, it could not be carried with sufficient confidence. Even for isopycnal T, a suggestion of higher eddy transport north of 44°N remains rather uncertain, and only the average of all the estimates for each survey will be discussed.

[41] For the surveys P1, P2, P3 which have adequate resolution, this average meridional eddy temperature transport is usually positive (northward) on all isopycnal surfaces. It is less by roughly a factor 3 for P3 than for the two other surveys, but the latitudinal range over which it could be estimated is not the same during P3. For σ_Θ = 27.10, this isopycnal eddy temperature transport averages 0.8 10^{-3} m s^{-1} °C. If only P1 and P2 are considered, this exceeds 1.0 10^{-3} m s^{-1} °C, as well as for other nearby sigma surfaces. A warm, oxygen-poor tongue spreads between P1 and P2 to the east of C4 and to at least 44°N. The current fields suggest northward advection of southern water that was bulging in this region during P1 south of 42°N. This feature, together with the colder more oxygenated water flowing to the south farther west contribute a large share of the meridional eddy transport during P1 and P2, and contribute to "age"/warm the newly formed waters of the northern part of the domain.

[42] The eddy transport is a down-gradient transport (Figure 3), as expected for eddy stirring. These values are rather uncertain, due to the RMS variability between the estimates at different latitudes, resulting in errors roughly on the order of 0.25 10^{-3} m s^{-1} °C. In addition, these eddy transports should be considered as underestimates of the real values, as the smoothing in the mapping process will result in a reduction of the contribution to the transport by the smaller scales. It was encouraging that similar results were obtained with estimates based on the mapped temperature from the data displaced with the currents to a common date (Appendix A). The direction of the eddy temperature fluxes is not similar to the one of the fluxes estimated (on a depth range) for this region by *Leach et al.* [2002] which was not found to be significantly nonzero. However, their estimate is not directly comparable to ours done on an isopycnal surface. Nonetheless, we also found in the upper 200 m layer a depth averaged eddy flux that has a northward meridional component (therefore an opposite direction to theirs).

[43] Assuming a Fickian formulation for the eddy transport, a diffusivity k can be estimated dividing the eddy temperature transport by the average gradients. Average diffusivity is found close to 2000 m^2/s, with smaller values during P3. This is in the range of estimates from one particle dispersion statistics of float data in a region west of the Iberian Peninsula [*Colas*, 2003]. This was updated for the POMME float data set with an average value close to 2500 m^2/s [*Le Cann et al.*, 2005], indicating also a meridional structure of the diffusivity in the POMME domain. These values can be compared with *Karsten and Marshall*'s [2002] formulation adopted in the Antarctic circumpolar region $k = -0.26\langle g/f \rangle > (h'^2)^{1/2}$, which corresponds to k = 1300 m^2 s^{-1} (the RMS variability of the dynamic height at 100 m averages 5 cm in the reanalyses of AR2005). There is also *Stammer*'s [1998] formulation that relates k to eddy kinetic energy (EKE) and an integral timescale (based on baroclinic instability parameterization [*Visbeck et al.*, 1997]). With their estimate of integral timescale based on altimetry and an average EKE (75 cm^2 s^{-1}), this results in k = 500 m^2 s^{-1}, which is considerably less, but is rather uncertain. The change we find in eddy temperature transport

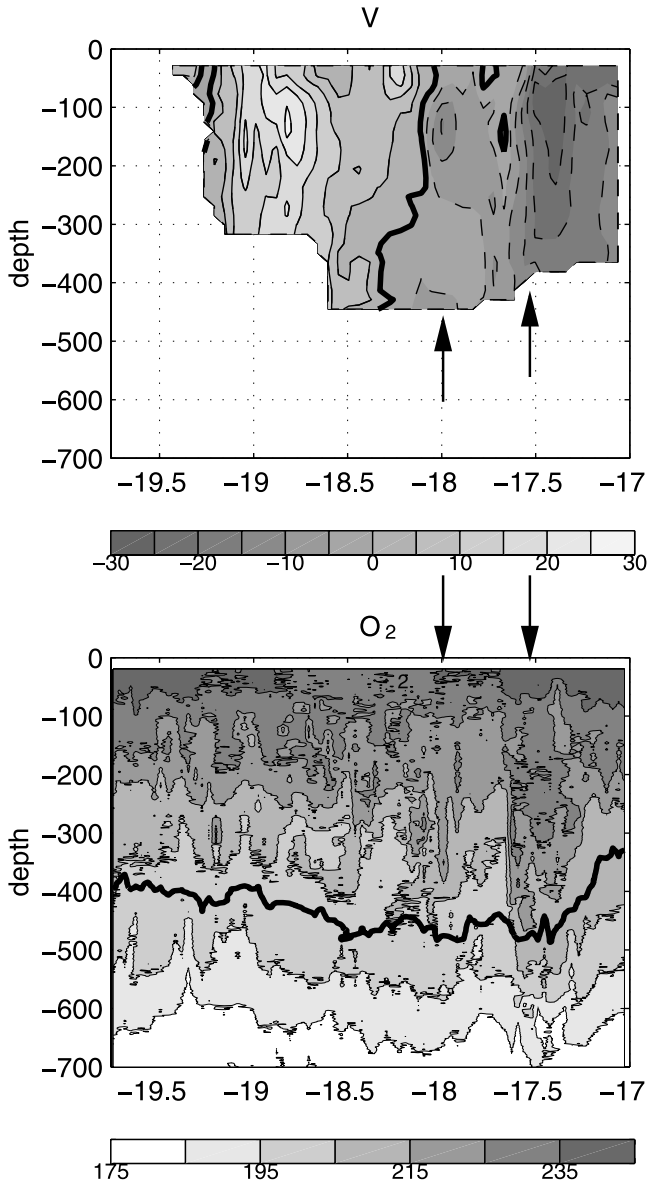

Figure 11. (top) Meridional velocity component section from the R/V *Atalante* vessel-mounted acoustic Doppler current profiler (VMADCP) (dashed southward; contours every 5 cm s^{-1}). (bottom) Oxygen from the high-resolution section from C4 (41.73°N, 19.78°W) to C5B (44.22°N, 17°W) during leg 2 of P2. The full line corresponds to the depth of T = 11.5°C (slightly below σ_Θ = 27.10). The arrows point to the positions of the largest isopycnal oxygen maxima on (σ_Θ = 27.05).

between P1, P2 on one hand, and P3 on the other, is also consistent with lower level of eddy activity during the last survey (AR2005) that should be associated with less eddy stirring.

[44] The values of eddy transports would induce large changes in the zonally averaged distributions if they were associated with a meridional structure of these transports. For example, for T, if the eddy transport was varying from 0 to the average value over the 3° between 38° and 41°N, it would contribute to an isopycnal cooling in that region of 0.04°C between P2 and P3. This has the magnitude of the changes observed between the surveys, which suggests the importance of eddy transports in the observed changes in average profile between the surveys. This seems however not sufficient to explain the changes between P1 and P2.

[45] It is also quite clear that the surveys had an insufficient resolution to properly map the mesoscale structures with a fairly large likely aliasing of the submesoscale structures of these scalar fields. This can be illustrated by dedicated high-resolution surveys during the leg 2 of P2. One was focused on the region to the east of A1 (near 17°W) which presented a low-temperature/high-oxygen signal during the leg 1 survey of that cruise (3 weeks earlier). A high-resolution section presented in this region two tongues with low stratification and high oxygen (Figure 11), the one farther east reminiscent of what is portrayed on the P2 maps. However, the transverse (near zonal) scale of that tongue is rather small (less than 50 km with features on the order of 10 km wide), and furthermore the southeastward current maximum is somewhat shifted with respect to the oxygen tongue according to the vessel-mounted acoustic Doppler current profiler (VMADCP) data (the largest currents being to the east of the oxygen maximum) (Figure 11). This suggests that correlation between velocity and oxygen was probably rather low in this case, and that mapping such property distributions at the mesoscales from a limited resolution survey can be associated with rather large errors. Indeed, the mapping of the first leg of P2 (3 weeks earlier) did not suggest at 42°N this spatial shift between velocity and temperature/oxygen extrema (Figure 7 presents a broad oxygen maximum).

6. Conclusions

[46] POMME illustrates the large-scale properties in ENAMW and its evolution that took place over the course of 1 year in the relatively quiescent region of the northeast Atlantic 38°–45°N where the field experiment took place. Some of these changes have been tracked to the late winter 2001 newly formed mode water (in particular in the northeast for the deeper sigma surfaces). Other changes have been found to result from advection by the horizontal currents and displacements of eddy structures. On the other hand, we found no evidence of spreading of these waters to the southern part of the domain, with instead suggestions that the changes in the south originated to some extent from water carried eastward near 41°–42°N, which origin cannot be determined with the POMME data.

[47] Interestingly, the large contrast in water masses found below at the SAIW-MSW levels (in the range $32.10 < \sigma_1 < 32.25$) has remained better preserved from P0 to P3 (not shown). This suggests a difference in the circulation between these two layers, as well as in the origin of the property gradients. Not surprisingly, in this deeper density range, the waters north of the eastward current have properties usually less influenced by the Mediterranean waters, which main source is southeast of the POMME domain.

[48] Furthermore, the surveys present clear evidence of stirring by the mesoscales, in particular in the central and northern part of the domain during P2: for example, the presence of tongue-like features in property distributions associated with northward or southward currents (or close to

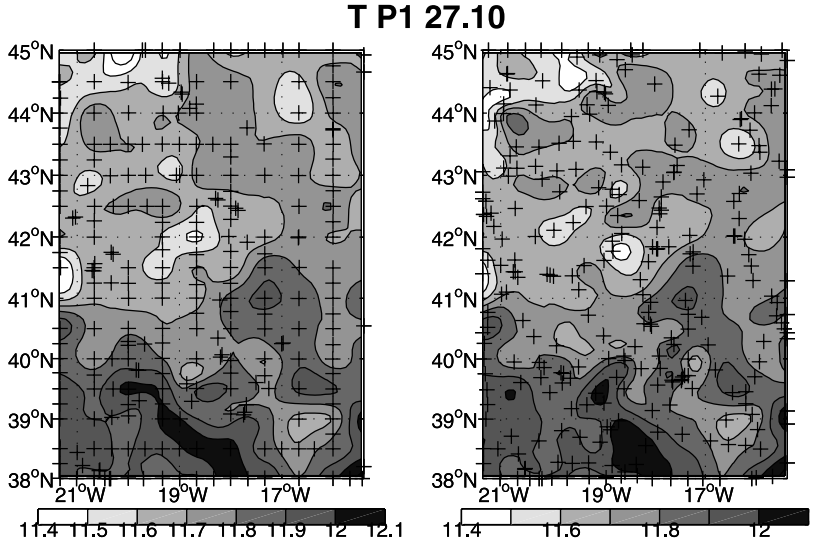

Figure A1. For P1 (σ_Θ = 27.10), comparison of the (left) standard *T* analysis with (right) one in which the data positions have been moved to a median date of the survey.

the currents) that suggest a meridional eddy transport by the mesoscales. This stirring by the currents was actually larger than expected, as EKE in the region in late 2000–early 2001 was larger than its climatological value estimated from altimetric data [*Volkov*, 2004]. This results in a large dispersion of trajectories and of the water masses, with only a small portion of what is found during one POMME survey still within the surveyed area 200 days later (as from P1 to P3, or even over 135 days from P0 to P1). This limits the extent to which we can interpret the large-scale changes in successive surveys, a note of caution that should be extended to the various biogeochemical properties that were measured during POMME.

[49] It should be also clear that the surveys marginally resolved the mesoscale variability. They are not synoptic and attempts to correct this effect by moving the station data as if they were advected by the currents to a common median date have sometimes resulted in somewhat different maps (Appendix A), although the large-scale properties remain nearly similar as well as the estimates of eddy transports. Higher-resolution surveys would be necessary to have reliable estimates of horizontal transports by the circulation, and to avoid the aliasing of the submesoscale features in these scalar fields. When integrating the trajectories over a longer time span (135 days between P0 and P1 or 155 days between P2 and P3), the results are also often not coherent with the observed changes in *T*, O_2 or N^2. The actual trajectory end points in these simulations are often very spread out after such a long integration time, indicative of a large stirring by the mesoscale field. It is likely that the accumulated errors are too large to provide quantitative tests with these fields. Probably, for these long integrations, one should only focus on the large-scale signals (for example, we find that C4 trajectories during P1 tend to originate from regions near 44°–45°N during P0). The simulated trajectories present comparable statistical properties (integral timescales (e.g., AR2005)). However, they often fail to reproduce the trapping of water in the core of eddies that has been witnessed by floats (for example in anticyclones A1 and A5 [*Le Cann et al.*, 2005]). The estimated error of these current analyses is also quite large (AR2005).

[50] The difficulty of investigating what causes the evolution of properties in this domain is that its size (500 km zonally by 750 km meridionally) is rather small compared to the displacements in 1 year witnessed by the POMME floats [*Le Cann et al.*, 2005]. This float data set suggests that less than 20% of the water initially in the domain in September 2000 was still present in the area surveyed in September 2001. The proportions are larger when considering the shorter periods separating the individual surveys.

[51] Further tests of the consistence of the data set will come from comparing the water mass properties observed in the spring (P2) with detailed analyses of mixed layer retreat [*Paci et al.*, 2005] and of water mass formation, both within the POMME domain, but also if possible in the neighboring regions. It will be also important to quantify how diapycnal diffusion affects properties on isopycnal surfaces (although we expect this effect to be small, as discussed by *van Aken* [2001]). Dissolved oxygen is also not a conservative tracer, with a large effect of respiration and remineralization on the deeper surfaces, in particular during the spring season. Estimates of these effects based on POMME data should be taken into account in the quasi-Lagrangian diagnostics (alternatively, one could combine nitrate and oxygen data in an appropriate fashion to have other quasi-conservative tracers).

Appendix A: Nonsynopticity of the Surveys

[52] As a simple way to test the effect on the analyses of the evolution during the duration of the surveys, we simulated trajectories in the analyzed velocity fields of AR2005 to move the data to the median date of the survey. According to *Rixen et al.* [2001], this should result in a more representative field. This is associated with a somewhat irregular set of positions for the moved data that are then analyzed in a similar way to what is done for the data at their original station positions. The differences in the

analysis can be large locally with individual extrema placed differently (Figure A1). However, the large-scale features are fairly similar, and meridionally averaged estimates of eddy temperature transport are also rather close to the ones done in our standard analysis in which stations are not moved (differences are less than 0.3 10^{-3} m s^{-1} °C, except for P0 on $\sigma_\Theta = 27.05$, and much smaller for P1 and P3). The nonsynopticity of the array is therefore not a major hindrance for the analysis we have presented. It indicates however clearly that some of the isolated structures we see could have been perceived differently, if the array had been truly synoptic. A really synoptic vision of the POMME area during the surveys can however probably not be reached by our approach, as the current analyses have rather large errors, and that it will be difficult to take carefully into account the vertical structure of the currents (all trajectories were considered at the same prescribed depth).

[53] **Acknowledgments.** Financial support for POMME was received from the French agencies CNRS, IFREMER, Meteo-France, and SHOM. The data used result from a joint effort by all the POMME participants supported by the very professional and dedicated work done by the crews of the R/V *Atalante*, *Thalassa*, and *d'Entrecasteaux*. Françoise Besset did the property mapping and is responsible for many figures. The analyses of the data were funded by grants from the French research programs PATOM and PROOF, and the project was managed by Laurent Mémery and Gilles Reverdin. The surface temperature analyses were kindly provided by Guy Caniaux and the VMADCP section by Pascale Lherminier.

References

Assenbaum, M., and G. Reverdin (2005), Near real-time analyses of the mesoscale circulation during the POMME experiment, *Deep Sea Res., Part I*, in press.

Bretherton, F. P., R. E. Davis, and C. B. Fandry (1976), A technique for objective mapping and design of oceanographic experiments, *Deep Sea Res.*, *23*, 559–582.

Caniaux, G., A. Brut, D. Bourras, H. Giordani, A. Paci, L. Prieur, and G. Reverdin (2005), A 1 year sea surface heat budget in the northeastern Atlantic basin during the POMME experiment: 1. Flux estimates, *J. Geophys. Res.*, *110*, C07S02, doi:10.1029/2004JC002596.

Colas, F. (2003), Circulation et dispersion Lagrangiennes en Atlantique nord-est, Ph.D. thesis 943, 253 pp., Univ. Bretagne Occidentale, France.

Cunningham, S. A. (2000), Circulation and volume flux of the North Atlantic using synoptic hydrographic data in a Bernoulli inverse, *J. Mar. Res.*, *58*, 1–35.

Ducet, N., P. Y. Le Traon, and G. Reverdin (2000), Global high-resolution mapping of ocean circulation from TOPEX/Poseidon and ERS-1 and -2, *J. Geophys. Res.*, *105*, 19,477–19,498.

Fernández, I. C., P. Raimbault, G. Caniaux, N. Garcia, and P. Rimmelin (2005), Influence of mesoscale eddies on nitrate distribution during the POMME program in the north-east Atlantic Ocean, *J. Mar. Syst.*, *55*, 155–175.

Harvey, J., and M. Arhan (1988), The water masses of the central North Atlantic in 1983–1984, *J. Phys. Oceanogr.*, *18*, 1855–1875.

Karsten, R. H., and J. Marshall (2002), Constructing the residual circulation of the ACC from observations, *J. Phys. Oceanogr.*, *32*, 3315–3327.

Leach, H., S. J. Bowerman, and M. E. McCulloch (2002), Upper-ocean eddy transports of heat, potential vorticity, and volume in the northeastern North Atlantic "Vivaldi 1991," *J. Phys. Oceanogr.*, *32*, 2926–2937.

Le Cann, B., M. Assenbaum, J.-C. Gascard, and G. Reverdin (2005), Observed mean and mesoscale upper ocean circulation in the midlatitude northeast Atlantic, *J. Geophys. Res.*, *110*, C07S05, doi:10.1029/2004JC002768.

Lévy, M., Y. Lehahn, J.-M. André, L. Mémery, H. Loisel, and E. Heifetz (2005), Production regimes in the northeast Atlantic: A study based on Sea-viewing Wide Field-of-view Sensor chlorophyll and ocean general circulation model mixed layer depth, *J. Geophys. Res.*, doi:10.1029/2004JC002771, in press.

Maixandeau, A., et al. (2005), Microbial community production, respiration, and structure of the microbial food web of an ecosystem in the northeastern Atlantic Ocean, *J. Geophys. Res.*, doi:10.1029/2004JC002694, in press.

Paci, A., G. Caniaux, M. Gavart, H. Giordani, M. Lévy, L. Prieur, and G. Reverdin (2005), A high-resolution simulation of the ocean during the POMME experiment: Simulation results and comparison with observations, *J. Geophys. Res.*, doi:10.1029/2004JC002712, in press.

Paillet, J., and M. Arhan (1996), Shallow pycnoclines and mode water subduction in the eastern North Atlantic, *J. Phys. Oceanogr.*, *26*, 96–114.

Paillet, J., and H. Mercier (1997), An inverse model of the eastern North Atlantic general circulation and thermocline ventilation, *Deep Sea Res., Part I*, *44*, 1293–1328.

Perez, F. F., A. F. Rios, B. A. King, and R. T. Pollard (1995), Decadal changes of the Θ-*S* relationship of the eastern North Atlantic Central Water, *Deep Sea Res., Part I*, *42*, 1849–1864.

Pollard, R. T., and S. Pu (1985), Structure and circulation of the upper Atlantic Ocean northeast of the Azores, *Prog. Oceanogr.*, *14*, 443–462.

Pollard, M. J., S. A. Cunningham, J. F. Read, F. F. Perez, and A. F. Rios (1996), A study of the formation, circulation and ventilation of eastern North Atlantic Central Water, *Prog. Oceanogr.*, *37*, 167–192.

Rixen, M., J. T. Allen, and J.-M. Beckers (2001), New synoptic versus pseudo-synoptic data sets: An assimilation experiment, *J. Mar. Syst.*, *29*, 313–333.

Stammer, D. (1998), On the eddy characteristics, eddy transports, and mean flow properties, *J. Phys. Oceanogr.*, *28*, 727–739.

Valdivieso da Costa, M., H. Mercier, and A.-M. Treguier (2005), Effects of the mixed-layer time variability on kinematic subduction rate diagnostics, *J. Phys. Oceanogr.*, *35*, 427–443.

van Aken, H. M. (2001), The hydrography of the mid-latitude northeast Atlantic Ocean. Part III: The subducted thermocline, *Deep Sea Res., Part I*, *48*, 237–267.

Visbeck, M., J. Marshall, T. Haine, and M. Spall (1997), On the specification of eddy transfer coefficients in coarse-resolution ocean circulation models, *J. Phys. Oceanogr.*, *27*, 381–402.

Volkov, D. L. (2004), Monitoring the variability of sea level and surface circulation with satellite altimetry, Ph.D. thesis, 152 pp., Univ. of Utrecht, Netherlands.

M. Assenbaum, Laboratoire d'Etudes en Géophysique et Océanographie Spatiales/Observatoire Midi-Pyrénées, Service Hydrologique et Océanographique de la Marine, 14 avenue Edouard Belin, F-31400 Toulouse, France. (michel.assenbaum@cnes.fr)

L. Prieur, Laboratoire d'Océanographie de Villefranche, Centre National de la Recherche Scientifique, BP 28, F-06234 Villefranche-sur-mer Cedex, France. (prieur@obs-vlfr.fr)

G. Reverdin, Laboratoire d'Océanographie Dynamique et de Climatologie, Institut Pierre-Simon Laplace, Centre National de la Recherche Scientifique, case 100, 4 pl. Jussieu, F-75252 Paris Cedex 05, France. (reverdin@lodyc.jussieu.fr)